Assessing Impact Damage In Thermoplastic Composites Using Maximum Contrast Approach

Pusan Dhar, Manoj Rijal, Richard Dela Amevorku, David Amoateng Mensah

(Mechanical Engineering, North Carolina A&T State University, USA)
(Mechanical Engineering, North Carolina A&T State University, USA)
(Mechanical Engineering, North Carolina A&T State University, USA)
(Mechanical Engineering, North Carolina A&T State University, USA)

Abstract:

Background*: With the widespread use of carbon fiber reinforced polymers (CFRP) in the aerospace industry, detecting damage or defects has become crucial in preserving the structural integrity of these systems.*

Materials and Methods*: This research aims to explore the effectiveness of thermography non-destructive evaluation (TNDE) in assessing impact damage in structural components of carbon/thermoplastic composites. Several coupons of carbon/thermoplastic composites impact damaged with a range of impact energy were inspected using active flash thermography. Thermal data obtained from thermography was processed using thermographic signal reconstruction, and the defect depth and size were estimated using a calibration profile and the maximum contrast approach. These results were also compared with results from ultrasonic C-scan.*

Results*: The results from thermography were found to be consistent with those from the C-scan. Furthermore, damage progression in impacted tensile specimens was also evaluated under increasing loads, with areas of damage being measured using a pixel-count method.*

Conclusion: *The depth and area measurements evaluated from TNDE were consistent with the C-scan analysis, which confirms a high degree of agreement.*

Key Word: *Aerospace; TNDE; defect detection; TSR; image processing.*

I.   Introduction

Thermographic nondestructive evaluation (TNDE) is a widely recognized technique for quickly and effectively assessing structures. This method, which includes both 'Active' and 'Passive' thermographic techniques, has significant practical implications for CFRP in the aerospace and materials science industry. In the "Active" technique, an external source stimulates the top surface of an object, while an infrared (IR) camera records images depicting the rate of change of IR radiation over different time frames due to the applied heat. Subsequently, these images are converted to a temperature versus time profile using an algorithm. If the object is defect-free, the heat will diffuse through its thickness at a consistent rate. However, if there is any delamination due to impact damage, the depth of the delamination can be assessed by examining the variation of temperature over time. This variation creates a difference in contrast of thermal images between the delamination and the undamaged area. Deeper delamination images may appear blurry due to lower contrast and a gradient in contrast from the center to the region beyond the edges, which is caused by lateral heat diffusion just above the surface of the delamination. Winfree et al. demonstrated that these issues can be addressed using a calibration specimen [1].

In the realm of pulsed thermal non-destructive evaluation (NDE), Vavilov et al. [2] provided a comprehensive summary of its physics and theoretical foundations for enhanced comprehension. Furthermore, an appropriate image processing technique is essential for extracting delamination-related information from the raw images captured by an infrared (IR) camera. Ibarra-Castanedo et al. discussed various data processing methods for defect detection and quantitative characterization [3]. Recent advancements in data processing have significantly improved the accuracy of defect detection in composite materials. The Thermographic Signal Reconstruction (TSR) technique stands out as a prominent pixel-based data processing method for enhancing defect detection. Shepard et al. [4] applied the TSR technique to an entire time sequence to generate a single image (TSR fingerprint), which can be valuable for comparing samples with a defect-free reference. Ciampa et al. [5] compared recently utilized data processing techniques, including TSR, for thermographic non-destructive evaluation (TNDE) of aerospace components to assess the effectiveness of these techniques.

This study introduces a new method for selecting the appropriate threshold value using the maximum contrast approach. This method will be useful for obtaining damage-related information in a comprehensive

---

manner, ensuring that no important damage-related information is overlooked. To validate this method, well-established C-scan results were compared, and consistent results were obtained after this comparison.

II. Background

In the Active thermographic technique, the surface of the object is stimulated by an external source. If the surface temperature of the object is raised by a uniform stimulation, then heat will be diffused only along the thickness, and for a semi-infinite body, the differential equation of heat conduction will be

$$\frac{\partial^2 T}{\partial z^2} - \frac{1}{\alpha}\frac{\partial T}{\partial t} = 0 \qquad (1)$$

Where z is the coordinate along the thickness direction, and α is the thermal diffusivity, which can be defined as

$$\alpha = \frac{K}{\rho C} \qquad (2)$$

Here K, ρ, and C are the thermal conductivity, density, and heat capacity, respectively.

Equation (1) is also valid for a finite thickness plate as there is no heat is generated internally. If we consider an insulated boundary condition, according to Carslaw and Jaeger [6], the solution of the differential equation (1) is given by

$$\Delta T = \frac{Q}{\varepsilon\sqrt{\pi t}} \qquad (3)$$

Where Q is the total heat provided at the surface as a flash, ΔT is the temperature difference of the surface at time 't' after the flash and initial temperature, and ε is the effusivity defined as

$$\varepsilon = \sqrt{K\rho C} \qquad (4)$$

Now, for a semi-infinite body, the temperature evaluation of the surface can be described better in a logarithmic scale. So, the natural logarithm of the equation (3) will be

$$\ln(\Delta T) = -0.5\ln(t) + \ln\left[\frac{Q}{\varepsilon\sqrt{\pi}}\right] \qquad (5)$$

If we plot ln (ΔT) versus ln (t) the slope of that plot has a value of negative 0.5. Any deviation from this value will indicate the presence of discontinuities of that material. Now, the main interest is the time of heat diffusion from one surface to the other surface of the object through thickness direction, as for a defect-free component, lateral heat diffusion will cancel out. The time at which the slope of the cooling curve deviates from the negative 0.5 will be used to locate the depth of the defect which can be expressed as

$$t = \frac{L^2}{\pi\alpha} \qquad (6)$$

Now, the Thermographic Signal Reconstruction (TSR) method was developed based on the straight-line behavior of the logarithmic temperature vs. time plot and the amplification of deviations from linearity [7,8]. This method uses a least-squares fit to match the logarithmic temperature response of each pixel to a low-order polynomial, resulting in a noise-free replica of the original data that allows for further processing without added noise [9]. This curve fitting tool acts as a low-pass filter, improving the signal-to-noise ratio (SNR).

To determine the best polynomial fit order, the Signal to Background Contrast (SBC) method was introduced as an alternative to SNR [10]. A higher SBC value indicates better signal quality and the best polynomial fit order. Thus, the fit order with a higher SBC value is used to convert the raw data set (raw image from thermographic camera) to a TSR data set, resulting in a TSR image. The logarithmic derivatives [1st (1D) and 2nd (2D)] of TSR amplify the effects of the interaction of applied heat with the subsurface interfaces. This enhancement allows for significant amplification of flaws or discontinuities in the object compared to the raw data set, facilitating quantitative flaw detection.

The Time Series Reconstruction (TSR) method can be used on the entire pixel time history to generate a single image, known as a 'TSR fingerprint,' which can be used to compare a sample to a defect-free zone. The shape of the curves in the fingerprint is useful for comparing automated sequences using statistical correlation. This comparison is independent of the orientation of the sample or its position in the field of view [4]. Examining the color map of these differently shaped curves makes it possible to determine a specific threshold value (figure 3b).

III. Methodology

Initially, several line profiles were randomly drawn on the thermographic image of impact damaged coupon (2''x12'') using a commercially available software named 'VIRTUOSO.' Subsequently, noise removal filtering and two median filters were applied to identify a background zone for calculating the signal-to-noise ratio (SNR). An alternative approach using Sripragash et al.'s [11] sound zone selection was also considered. The curve with the lowest intensity was then chosen to represent the respective background and marked as a black circle Figure 1.

The most suitable polynomial fit order results in the highest signal-to-noise ratio (SNR) values. VIRTUOSO is employed to attain the optimal SNR value for determining the perfect polynomial fit order. The SNR calculation involves considering an 8x8 pixel box (0.002 m * 0.002 m) for both the target and the

background. SNR values were analyzed for fit orders ranging from 1 to 15. Among them, fit order 7 exhibited the highest SNR values and was therefore selected for TSR.
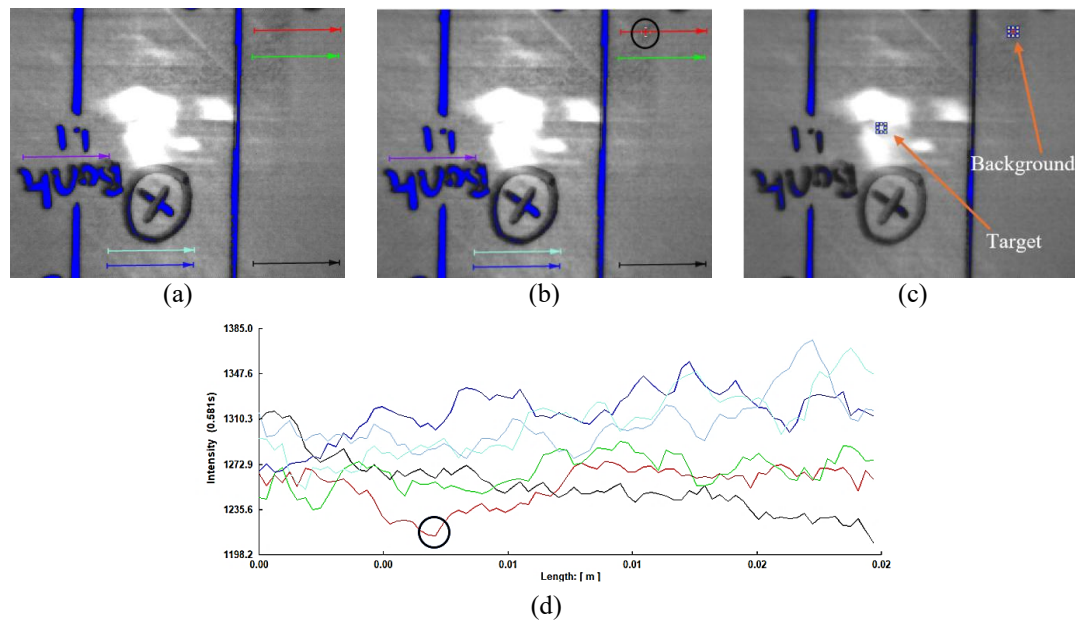
Figure 1 (a) Thermographic line profile (b) Sound zone selection (black circle) (c) Background and Target selection for SNR measurement (d) Intensity of pixels along thermographic line profile.
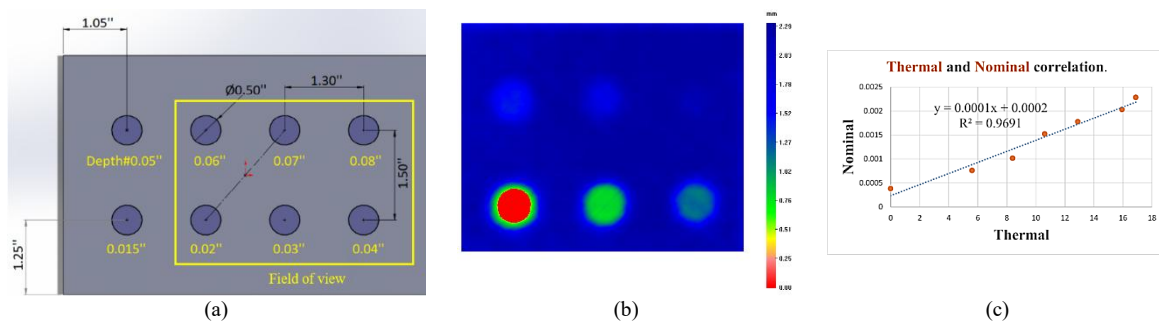
Figure 2. (a) FBH with different known depths, (b) Thermographic image of FBH for calibration, and (c) Thermal and nominal correlation viewgraph.

A predominantly pristine composite plate (thickness: 2.286 mm) with similar thermal properties was chosen in the depth determination process. Subsequently, eight flat-bottom holes of the same diameter but varying in depth from the surface were created on the plate (Figure 2a). Thermographic images were then captured and used to establish a calibration profile (Figure 2b). This profile was developed based on the correlation between thermal and nominal data and then applied to measure the depth of impact damage on similar plates with the same properties using the transfer function (Figure 2c).

Table 1. SNR values of respective fit order

| Fit Order	Raw (SNR)	TSR (SNR)
6	97.43	100.94
7	97.43	101.72
8	97.43	100.57
9	97.43	100.18
10	97.43	98

Thresholding is a technique for creating binary images that separate regions or objects of interest from the background based on intensity or color. By setting a threshold value, pixels in the image can be classified as foreground (object of interest) or background (non-object) based on whether their intensity values exceed or fall below the threshold. Setting a threshold value can help to avoid the contrast, which is related to lateral heat diffusion.

Figure 3 shows a graphic representation and contour plots of the first logarithmic derivatives (1D) of TSR. To set the threshold, 1D contour plots (TSR fingerprint) generated by VIRTUOSO were used.

(a)   (b)
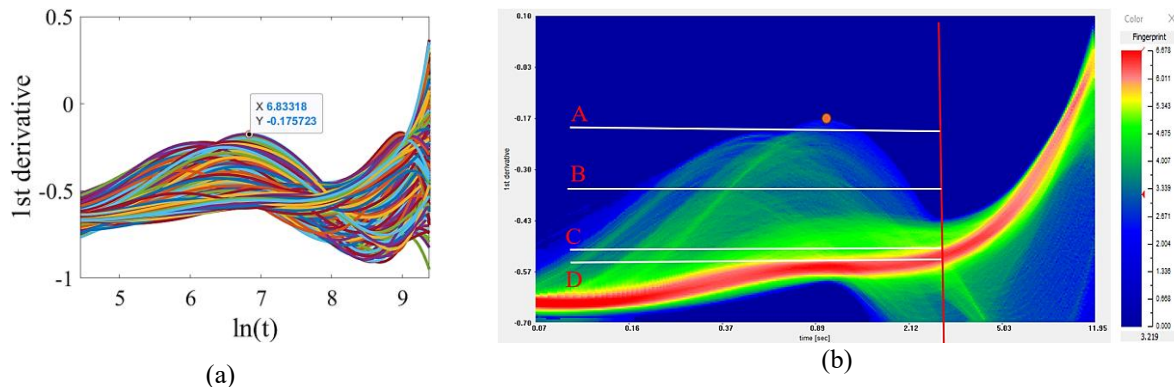
Figure 3. Graphical representation (a) and contour plots (b) of the first logarithmic derivatives (1D) of TSR

The red zone represents the temperature decay curve of pixels related to the sound zone, while the orange dot indicates the highest peak of the temperature decay curve, which can be considered as the center of a larger defect where heat cannot dissipate for a long time. The red vertical line indicates a specific time frame (517: 3.452 s) beyond which there is a possibility of no existence of damage or defect-related information, as there are no peaks after that. Up to the 517th frame is considered to ensure that no defect-related curve peaks are missed. Threshold values were selected step by step to generate different images of classified pixels and analyze the information.

(a)   (b)   (c)   (d)
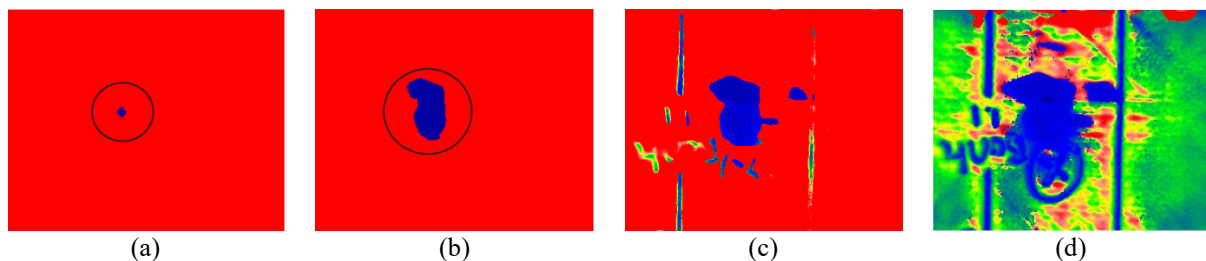
Figure 4. Schematic diagrams of classified pixels with different threshold values.

In the first step, a threshold value of -0.192 (A) and a time frame of 517 were chosen based on fingerprint analysis. This selection resulted in the identification of an image containing classified pixels, as shown in Figure 4a. The image shows that the gradient in contrast of pixels in the central region corresponds to significant delamination as the highest peak (topmost peak, indicated by an orange dot) among temperature decay curves. This peak suggests the time at which the temperature of those pixels in the central region starts to decrease due to lateral heat diffusion. Subsequently, a threshold value of -0.336 (B) and time frame 517 were considered, resulting in the generation of Figure 4b. This image represents the contrast of classified pixels away from the center region and the contrast of classified pixels in the center region of different damages at different depths. Following this, the threshold value of -0.472 (C) and time frame 517 were selected, yielding the result shown in Figure 4c. This image includes the contrast of classified pixels belonging to mostly all the damages at different depths. Finally, the threshold value of -0.54 (D) and time frame 517 were selected, and an image similar to Figure 4d was generated. This image includes the contrast of classified pixels belonging to all damage, subsurface defects, or voids, including the pixels of defect-free zones. Analyzing such an image in search of internal impact damage is challenging.

Our primary objective was to obtain information about the internal impact damage. Thus, this impact-damaged sample's threshold value of -0.472 (C) was selected for further analysis.

After adjusting the threshold value, the calibration profile was applied to the found image using a transfer function. After calibration, figure 5a displays the depth map of selected pixels corresponding to the impact damage zone. The color bar indicates the depth scale in accordance with the contour plot. The viewgraph (figure 5b) shows the corresponding time-temperature deviation curves of those selected pixels from the sound zone curve (A).

After adjusting the threshold values and frames, thermographic images were utilized to measure the areas of impact damage. The pixel-counting method was used for this purpose. The field of view contained

320x256 pixels. Subsequently, a ruler was employed to measure the field view area, which was equivalent to 83.515x66.776 units. MATLAB was utilized to measure the region of interest (ROI) for each thermographic image. The scaling of the captured image area is represented in Figure 6.

(a)   (b)
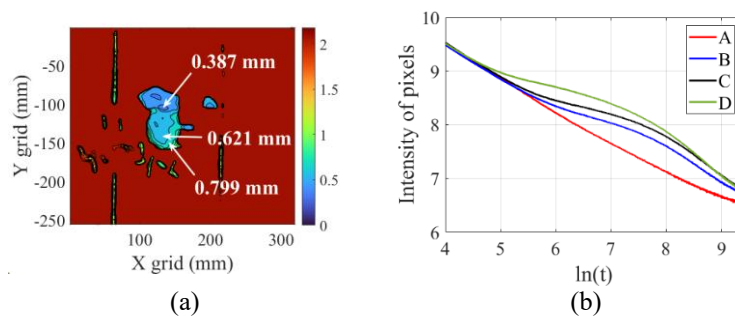
**Figure 5**. (a) Depth map. (b) Temperature-time deviation curves of selected pixels

(a)   (b)   (c)
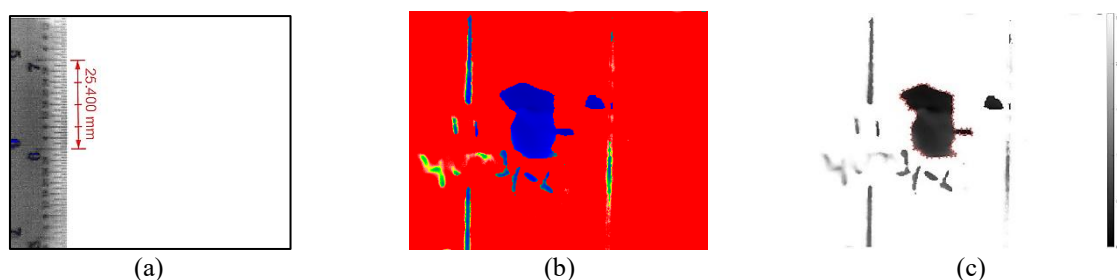
Figure 6. (a)Scaling (b) Image obtained from thermography (c) Image converted to gray scale for area measurement.

IV. Results And Discussion

The primary objective of this research was to identify specific information related to the damage. To achieve this, a Region of Interest (ROI) was chosen in each thermographic image for focused data processing. Figures 7a and 7d display the raw images of a sample captured by an IR camera on both sides, with the ROI highlighted by a red rectangle.

Subsequently, a depth map was constructed to adhere to the study's methodology, and three pixels were selected to annotate the depth accordingly (figure 7b, 7e). Figures 7c and 7f present the ultrasonic C-scan of the sample on both sides, conducted by QARBON AEROSPACE (measurements are in inches). Notably, exact pixel selection in thermographic images is challenging compared to in C-scans. The selected pixels in the thermographic depth map indicate depth values close to those of the adjacent pixels shown in the C-scan. Furthermore, Figures 8 and 9 illustrate the comparison of depth values between thermographic evaluation and ultrasonic C-scan.
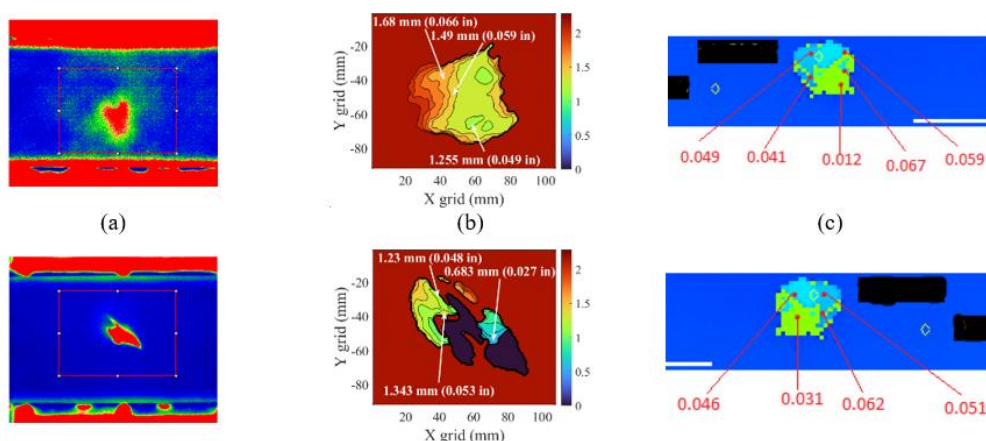

Figure 7. (a) Raw image of the front side of a specific sample (b) Depth map of the front side (c) C-scan of the front side (d) Raw image of the rear side of that sample (e) Depth map of the rear side (f) C-scan of the rear side.

Area measurements were carried out using the pixel counting method and compared with the results from the C-scan. The estimated area by TNDE was found to be consistent with the C-scan results. It should be emphasized that obtaining a clear image of deeper defects or damage in active thermography is challenging due to lateral heat diffusion on the surface just above the defect. Consequently, thermographic images were captured from both sides and compared for area measurement, and the side where the largest damaged region was identified was considered. The thermographic images were then converted in accordance with the grayscale to find the edge of an impact properly. Some other regions looked like damage, but these are the voids or pores inside the composite sample. Table 2 showcases the area measurement and the comparison of the measured area by thermography and C-scan.
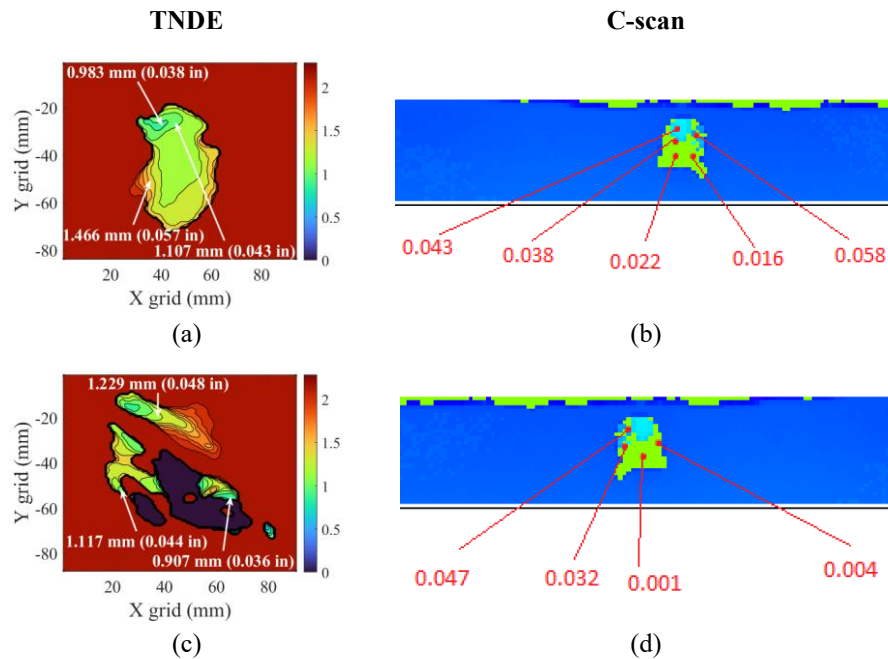
Figure 8. Depth estimation and the comparison of the estimated depth by thermography and C-scan for a 2"x12" tensile coupons. (a) Thermogram with depth map from impact side. (b) C-scan from impacted side. (c) Thermogram with depth map from opposite surface (d) C-scan from opposite surface.
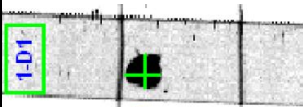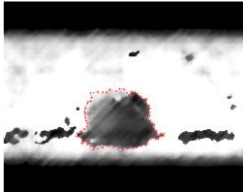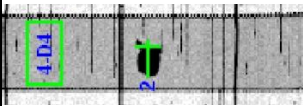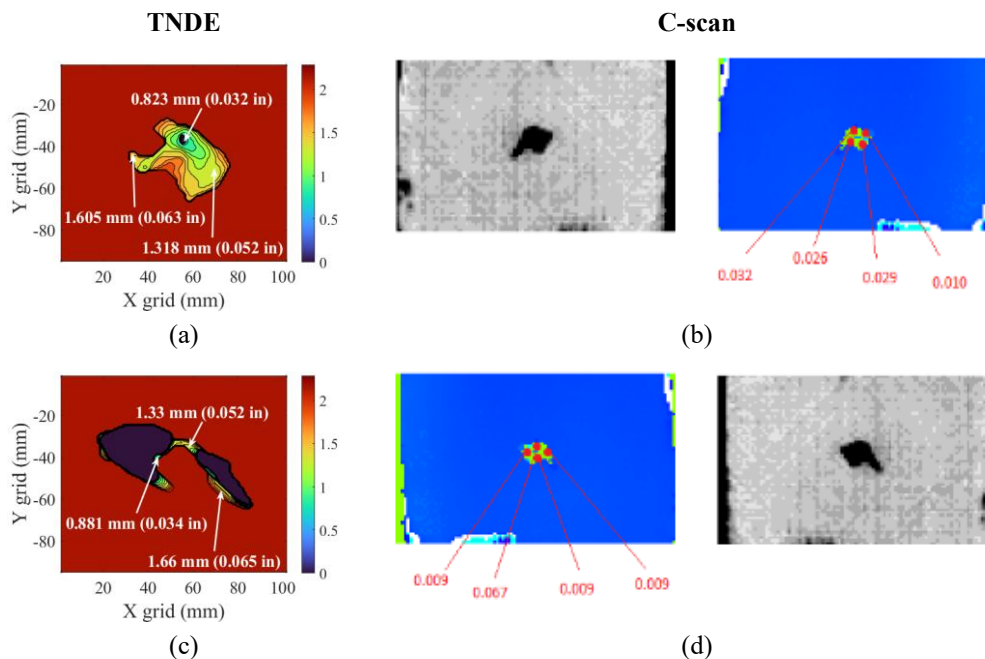

Figure 9. Depth estimation and the comparison of the estimated depth by thermography and C-scan for a 4" x 6" plate. (a) Thermogram with depth map from impact side. (b) C-scan from impacted side. (c) Thermogram with depth map from opposite surface (d) C-scan from opposite surface.
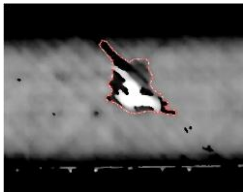
The values of area measurement are dependent on several factors. Firstly, frame selection is crucial in capturing the edge of the impact damage area within the sample. While the frame can be predicted using TSR fingerprint, obtaining the actual frame representing the heat diffusion from the edge of the impact damage region when viewed from the top surface remains challenging. Another critical factor is the depth of the damaged area. In C-scans, the overall damage area through the full thickness is precisely defined with a sharp edge, whereas in thermography, damage closer to the surface can be easily detected due to its higher contrast, but deeper damage appears blurred. This phenomenon is primarily attributed to lateral heat diffusion just above the deeper damage or defect.

As a result, a contrast gradient is typically generated from the center to the regions beyond the edges of the damage, making it difficult to obtain a sharp edge. Furthermore, selecting the appropriate threshold value is crucial to differentiate between the contrast of pixels related to voids/pores and impact damage.

Thermographic images were captured before and during the tensile test at various loads to observe the progression of damage in impacted tensile specimens under increasing load (figure 10). It was observed that there was an enlargement of the impact damage area on the rear side, while there was no significant change on the front side, except for a load of 10000 pounds. This difference may be attributed to the presence of a large number of voids or pores near the surface of the rear side.

Table 2. Area measurement and the comparison of the measured area by thermography and C-scan

Impact Energy	C-scan area (mm²)	Thermography area (mm²)	Difference	Percentage of error
14.56 J	419.078	434.671	-15.593	-3.72
14.62 J	322.471	300.900	21.571	6.69

This study estimated depth and damage sizes using the calibration profile and TSR fingerprint, respectively. It is difficult to fabricate actual calibration specimens' representation of the variety of impact damages encountered in practice. A normalization procedure enables direct comparison of numerically generated thermal responses of such a variety of delamination and can potentially serve as a substitute for calibration specimens. This approach can be utilized in creating a dataset of impact damage for different loads in future works.

V. Conclusion

In this particular research study, a novel approach is presented for the selection of an optimal threshold value by employing the maximum contrast method. The study found that the estimated depth and area obtained through TNDE were in agreement with the results obtained from C-scan analysis, indicating a high level of consistency. Moreover, the authors utilized thermographic imaging techniques to capture images both before and during the application of varying loads during the tensile test. This was done to closely observe and analyze the evolution of damage in tensile specimens impacted at different load levels.
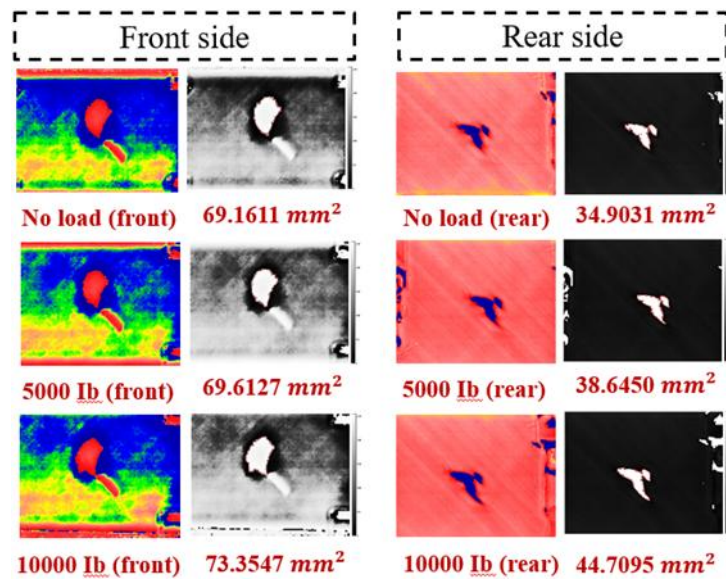
Figure 10. Damage progression in impacted tensile specimens under increasing load

Acknowledgement

References

[1]. Winfree, W. P., & Zalameda, J. N. (2003, April). Thermographic Determination Of Delamination Depth In Composites. In Thermosense XXV (Vol. 5073, Pp. 363-373). SPIE.

[2]. Vavilov, V. P., & Burleigh, D. D. (2015). Review Of Pulsed Thermal NDT: Physical Principles, Theory And Data Processing. Ndt & E International, 73, 28-52.

[3]. Ibarra-Castanedo, C., Gonzalez, D., Klein, M., Pilla, M., Vallerand, S., & Maldague, X. (2004). Infrared Image Processing And Data Analysis. Infrared Physics & Technology, 46(1-2), 75-83.

[4]. Shepard, S. M., Lhota, J. R., Hou, Y., Ahmed, T., & Wang, D. (2004). Thermographic Characterization Of Composite Materials And Structures. In Proceedings Of The International SAMPE Symposium And Exhibition (Vol. 49, Pp. 1953-1959).

[5]. Ciampa, F., Mahmoodi, P., Pinto, F., & Meo, M. (2018). Recent Advances In Active Infrared Thermography For Non-Destructive Testing Of Aerospace Components. Sensors, 18(2), 609.

[6]. Carslaw, H. S., & Jaeger, J. C. (1939). On Green's Functions In The Theory Of Heat Conduction.

[7]. Shepard, S. M., Lhota, J. R., Rubadeux, B. A., Wang, D., & Ahmed, T. (2003). Reconstruction And Enhancement Of Active Thermographic Image Sequences. Optical Engineering, 42(5), 1337-1342.

[8]. Shepard, S. (2013). U.S. Patent No. 8,449,176. Washington, DC: U.S. Patent And Trademark Office.

[9]. Shepard, S. M. (2018). Surface-Excited Thermography.

[10]. Gruber, J., Gresslehner, K., Sekelja, J., Mayr, G., & Hendorfer, G. (2014, November). Signal To Noise Ratio Threshold In Active Thermography. In 6th International Symposium For NDT In Aerospace (P. 8).

[11]. Sripragash, L., & Sundaresan, M. (2017). Non-Uniformity Correction And Sound Zone Detection In Pulse Thermographic Nondestructive Evaluation. Ndt & E International, 87, 60-67.